J. Electrochem. Sci. Eng. **16** (2026) 3222; https://doi.org/10.5599/jese.3222

Open Access : : ISSN 1847-9286
https://pub.iapchem.org/ojs/index.php/JESE

Original scientific paper

Carboxylate-controlled electron transfer in *Bacillus clausii* J1G-0%B halophilic microbial fuel cells

Marcelinus Christwardana[1,2,3,✉], Aprilia Budiarti[1] and Mukhammad Asy'ari[1]

[1]*Department of Chemistry, Faculty of Science and Mathematics, Diponegoro University, Indonesia*
[2]*Master Program of Energy, School of Postgraduate Studies, Diponegoro University, Indonesia*
[3]*Research Collaboration Center for Electrochemistry, BRIN - UNDIP, Indonesia*

Corresponding Author: ✉ marcelinus@lecturer.undip.ac.id

Received: January 17, 2026; Accepted: April 30, 2026; Published: May 21, 2026

Abstract

Microbial fuel cells (MFCs) provide a cohesive approach to treating hypersaline wastewater and generating renewable energy. This research assessed the efficacy of halophilic Bacillus clausii J1G-0%B supplemented with acetate, lactate, or citrate at doses of 10, 30 and 50 mM. The half-cell investigation included cyclic voltammetry, diagnostics of the rate-determining step, electron transfer rate constant (k_s), pH profiles, and ammonia buildup. Comprehensive cell testing, including assessments of output voltage, peak power density, and biofilm mass, was also performed. In comparison to the control, all carbon sources enhanced the electrochemical response by 184.56 to 378.23 %, due to bacterial-electrode electron transfer, diffusion-limited kinetics, and the involvement of cytochromes a_3, b, c and/or c_1 in B. clausii. The MFC system generated an average voltage ranging from 33.64 to 77.87 mV and achieved a maximum power density between 19.19±3.11 and 58.16±3.54 mW m^{-2}. Within the tested range, the highest acetate concentration (50 mM) produced the largest electrochemical response, yielding k_s of 1.888±0.002 s^{-1}, an average voltage of 486.94 mV, and a power density of 58.16±3.54 mW m^{-2}. The results demonstrate that targeted carboxylate supplementation significantly improves electron transport and energy recovery in high-salinity microbial fuel cells, underscoring its viability for waste cleanup and energy generation during energy shortages and environmental contamination.

Keywords

Salty wastewater; bioelectricity generation; halophilic bacteria; carboxylate supplementation; biofilm growth; electron transfer kinetics

Introduction

Saline wastewater, such as that generated by the fish and seafood sector, poses a considerable global environmental concern due to its elevated organic load and salinity, which may impair the efficacy of traditional biological processes [1]. Microbial fuel cells (MFCs) have emerged as a

promising bioelectrochemical method for treating saline wastewater while simultaneously recovering renewable electrical energy, providing an integrated solution for pollution management and sustainable energy generation [2-4]. Nonetheless, the performance of MFCs under elevated salinity conditions is constrained by reduced electron-transfer efficiency, increased internal resistance, and erratic bioelectrocatalytic activity. A study by Vijay *et al.* [5] showed that halophilic anodes produced more power than freshwater bacteria-based anodes when supplied with saltwater, thereby supporting the use of halophilic microorganisms in harsh settings. Halophiles such as *Bacillus clausii* J1G-0%B, extracted from Madura salt ponds devoid of bittern fractions, exhibit physiological adaptations that facilitate growth and metabolic processes at elevated salt concentrations, which usually suppress standard electrogenic bacteria [6]. While bacilli are not often classified as classical electrogenic bacteria, several studies indicate that some strains may produce c-type cytochromes involved in extracellular electron transport. Although the salt resistance of these strains has been extensively researched, a thorough assessment of their electron transport dynamics in MFC setups remains notably scarce.

Research pertaining to *B. clausii*-based MFCs has been increasing. Recent studies have examined the influence of different salinity levels on the performance of *B. clausii* in MFCs, with optimal performance observed at 10% w/v NaCl [7]. Additionally, other research indicates that the incorporation of various nitrogen sources also impacts the electrobiological activity and electrical output of *B. clausii*-based MFCs [8]. Consequently, an unexplored research area is the function of carbon sources, especially simple carboxylates, in regulating electron transport and biofilm development in halophilic microbial fuel cell systems.

The availability of substrates is a crucial determinant of the operating efficiency of MFCs. Acetate and lactate are basic fermentation byproducts and electron donors often used by diverse anodic bacteria, facilitating a direct metabolic route to proton and electron production for current generation [9]. Sodium citrate has been shown to enhance electrical output and coulombic efficiency [10]. While these carboxylates have been thoroughly assessed in traditional MFC systems, research on their impact on halophilic electrogenic bacteria, namely *B. clausii* J1G-0%B, is scarce. The impact of varying carbon source concentrations on electron transfer kinetics, biofilm formation, and electrochemical performance in high-salinity environments remains inadequately understood.

Due to the reduced power production and instability of MFC activity in hypersaline environments, strategies to sustain microbial metabolism and enhance anodic electron transfer are critically required. Supplementation with basic carboxylates such as acetate, lactate, or citrate provides an effective means to improve carbon availability and bioelectrocatalytic stability. Nonetheless, most prior research has focused on freshwater or low-salinity environments, thereby limiting its applicability to halophilic MFCs.

The management of high-salinity wastewater faces two principal challenges: osmotic pressure, which limits microbial proliferation, and the limited supply of electron donors that can be effectively used for extracellular respiration. Carboxylates, including acetate, lactate, and citrate, are organic metabolites often present in diverse high-salinity industrial effluents, such as those from fermentation, food and beverage, and chemical manufacturing. These chemicals serve as readily biodegradable substrates for halophilic bacteria and provide electron donors via catabolic routes directly associated with the cell's electron transport chain. In current-generating bacteria, carboxylates may augment the synthesis of endogenous redox mediators, improve electron transfer to the anode surface, and regulate cellular metabolism under hyperosmotic circumstances.

Consequently, using carboxylates as an alternative carbon source may augment the efficacy of saline wastewater bioremediation and improve the electrogenic performance of MFCs.

This study investigates the influence of acetate, lactate, and citrate supplementation (10, 30 and 50 mM) on the electrochemical performance of microbial fuel cells (MFCs) employing *Bacillus clausii* J1G-0%B under hypersaline conditions (10 % w/v NaCl). While acetate is widely used as a model substrate in MFC research, quantitative electrochemical-biological analyses under hypersaline environments remain limited, and the extracellular electron transfer (EET) kinetics of halophilic bacteria have not been systematically resolved. The present work advances the field in three key aspects. First, it provides the first systematic evaluation of specific carboxylates as regulators of EET in halophilic *B. clausii*. Second, it integrates half-cell electrochemical kinetic analysis, *via* Laviron-derived heterogeneous electron transfer rate constants (k_s) and rate-determining step diagnostics, with full-cell MFC performance metrics, thereby establishing a mechanistic connection between interfacial electron transfer kinetics and device-level power output. Third, it quantitatively correlates k_s, maximum power density (MPD), and biofilm characteristics to demonstrate that electrochemical efficiency, rather than biomass accumulation alone, governs system performance under hypersaline stress. By combining electrochemical kinetics, full-cell performance evaluation, and metabolic indicators (pH variation and ammonia production), this study provides new insights into how carboxylate substrates regulate electron transfer pathways in halophilic MFC systems.

Experimental

Materials

The halophilic bacterium *Bacillus clausii* J1G-0%B, previously isolated from Madura salt ponds [6], was used as the inoculum. Culture media components included NaCl (Pudak Scientific), tryptone (Merck), yeast extract (Merck), $MgSO_4 \cdot 7H_2O$ (Merck), KCl (Merck), and $FeCl_3$ (Merck). Acetic acid, lactic acid, and citric acid (all Merck, analytical grade) were used as supplementary carbon sources, while NaOH (Merck) was applied for pH adjustment. Trisodium citrate (Merck) was included as a buffering agent, and an ammonia reagent kit (Monitor) was used to support analyses. All solutions were prepared with distilled water.

Cultivation of halophilic bacteria

The halophilic bacterium *Bacillus clausii* J1G-0%B was cultivated in a liquid halophilic medium containing 5 % (w/v) NaCl, 0.05 g tryptone, 0.025 g yeast extract, 1.0 g $MgSO_4 \cdot 7H_2O$, 0.15 g KCl, 0.15 g trisodium citrate, and 0.018 g $FeCl_3$ per 50 mL of distilled water [6]. The medium was sterilized by autoclaving at 121 °C for 15 min before use. This basal medium was used for bacterial pre-culture and half-cell experiments.

A single colony from a slant agar stock was inoculated into 50 mL of sterile halophilic medium and incubated at 37 °C with shaking at 150 rpm until the optical density (OD_{600}) reached 0.5 McFarland, which served as the inoculum. 1 vol.% of this inoculum was transferred into 50 mL of fresh halophilic medium and cultured under the same conditions. OD_{600} was measured every 8 h for 72 h using a UV-Vis spectrophotometer to monitor bacterial growth. After 72 h, the culture was supplemented with fresh halophilic medium with a modification of 10 w/v NaCl, and one of the carboxylate substrates (acetate, lactate, or citrate at 10, 30 or 50 mM). In this process, 10 % w/v NaCl created hypersaline conditions in the culture, and the process was run as fed-batch. The pH was adjusted to neutrality with 2 M NaOH, and the final volume was brought to 100 mL. Growth was monitored for an additional 5 days at 8-h intervals to establish growth curves under each carbon

source condition. The initial concentration of the culture followed the 0.5 McFarland standard, or equivalent to an absorbance of 0.08 to 0.1 at a wavelength of 600 nm (visible range).

For electrochemical experiments, a 1 vol.% inoculum was transferred into 50 mL of halophilic medium and incubated at 37 °C with shaking at 150 rpm for 72 h. The culture was then supplemented with fresh medium (50 mL) containing NaCl (7.5 g), tryptone (0.1 g), yeast extract (0.05 g), and one of the carbon sources (acetate, lactate, or citrate at 10, 30, or 50 mM). The pH was adjusted to neutrality, resulting in a total volume of 100 mL. These cultures were subjected to half-cell electrochemical measurements at t = 0 h and t = 72 h, followed by analysis of pH and ammonia concentration.

Half-cell electrochemical analysis

Electrochemical characterization of *Bacillus clausii* J1G-0%B cultures supplemented with acetate, lactate, or citrate was conducted using a single-chamber, three-electrode configuration. A glassy carbon disk (working electrode, WE), Ag/AgCl (reference electrode, RE), and stainless steel (counter electrode, CE) were immersed in the bacterial suspension within a Schott flask connected to a potentiostat (Rodeostat, USA). Cyclic voltammetry was performed to evaluate the electron transfer behaviour of bacterial cultures before and after incubation. Measurements were conducted within a potential window of -1.0 to +1.0 V *vs*. Ag/AgCl, with an initial scan rate of 0.1 V s^{-1}. To further probe electron transfer kinetics, post-incubation scans were conducted at varying rates from 0.1 to 1.6 V s^{-1} [11]. Current density was normalized to electrode surface area, and redox peak positions and intensities were extracted for subsequent analyses. The rate-limiting process was evaluated by plotting peak current density (j_p) obtained from CV against the applied scan rate (ν). Linearity of j_p vs. ν indicated a surface-controlled electron transfer, whereas deviation suggested diffusion-controlled processes. The heterogeneous electron transfer rate constant (k_s) was calculated using Laviron's method [12]. Briefly, the relationship between peak potential separation (ΔE_p) and log ν was fitted according to Laviron's equation to estimate k_s values, assuming quasi-reversible electron transfer conditions.

Metabolic byproducts were monitored by measuring culture pH using a calibrated pH meter. Ammonia concentrations were determined using a commercial ammonia detection kit (Monitor, Indonesia), with results expressed in ppm based on colorimetric calibration. These analyses provided supporting evidence of microbial metabolic activity under different carbon source conditions.

Full-cell experimental setup and analysis

Full-cell experiments were conducted to evaluate the effect of acetate, lactate, and citrate supplementation on the performance of MFCs inoculated with *Bacillus clausii* J1G-0%B. Bacterial cultures prepared as described in the previous section were used as anolytes in custom-built single-chamber polyacrylic MFC reactors (working volume 28 mL). Carbon felt electrodes (diameter 5 cm, thickness 0.5 cm) were employed as both anode and cathode materials, separated by a Nafion® 117 proton exchange membrane (DuPont). The reactors were operated under fed-batch conditions at 27 to 30 °C.

Cell voltage was continuously recorded across an external resistance of 1 kΩ using a digital multimeter (UNI-T UT61E) connected to a data acquisition system. Each cycle was operated for 72 h, and the experiment was repeated over three successive cycles. Voltage-time profiles were used to assess the stability and reproducibility of power generation under varying carbon-source conditions. Following the final cycle, polarization experiments were performed by varying external resistances from 10 MΩ to 10 Ω. The current (I) was calculated from Ohm's law ($I = V/R$), and the corresponding power (P) was obtained from $P = IV$. Power density was normalized to the projected anode surface area. Maximum power density (MPD) was determined from the peak of the power density *vs.* current density curve [13].

Biofilm formation on the anode was assessed by comparing the mass of carbon felt electrodes before and after MFC operation. Prior to use, anodes were dried at 60 °C to constant weight and the initial mass was recorded. After the operation, electrodes were carefully removed, gently rinsed with sterile 0.9% NaCl solution to remove loosely attached salts and planktonic cells, and dried again under the same conditions before re-weighing. The difference between the final and initial mass was attributed to biofilm accumulation on the electrode surface.

Statistical analysis

All measurements were performed in triplicate, and the results are reported as mean ± standard deviation

Results and discussion

Analysis of the growth curve for Bacillus clausii J1G-0%B

The growth curve of *Bacillus clausii* J1G-0%B, supplemented with acetate, lactate, and citrate, was assessed by measuring optical density at 600 nm wavelength (OD_{600}) in a fed-batch system [14], using UV-Vis Shimadzu UV-1280 (Kyoto, Japan). The two-stage development seen in the control culture (Figure 1a) included stage 1 with halophilic medium and stage 2 with modified halophilic media, characterized by an initial lag phase (~ 0 to 8 h), exponential growth lasting up to 48 hours, and a stationary phase extending to 72 h. Following the introduction of the new medium at 72 h, the bacteria resumed the logarithmic phase, with a brief acclimatization period, and subsequently reached the stationary phase by 144 h [15].

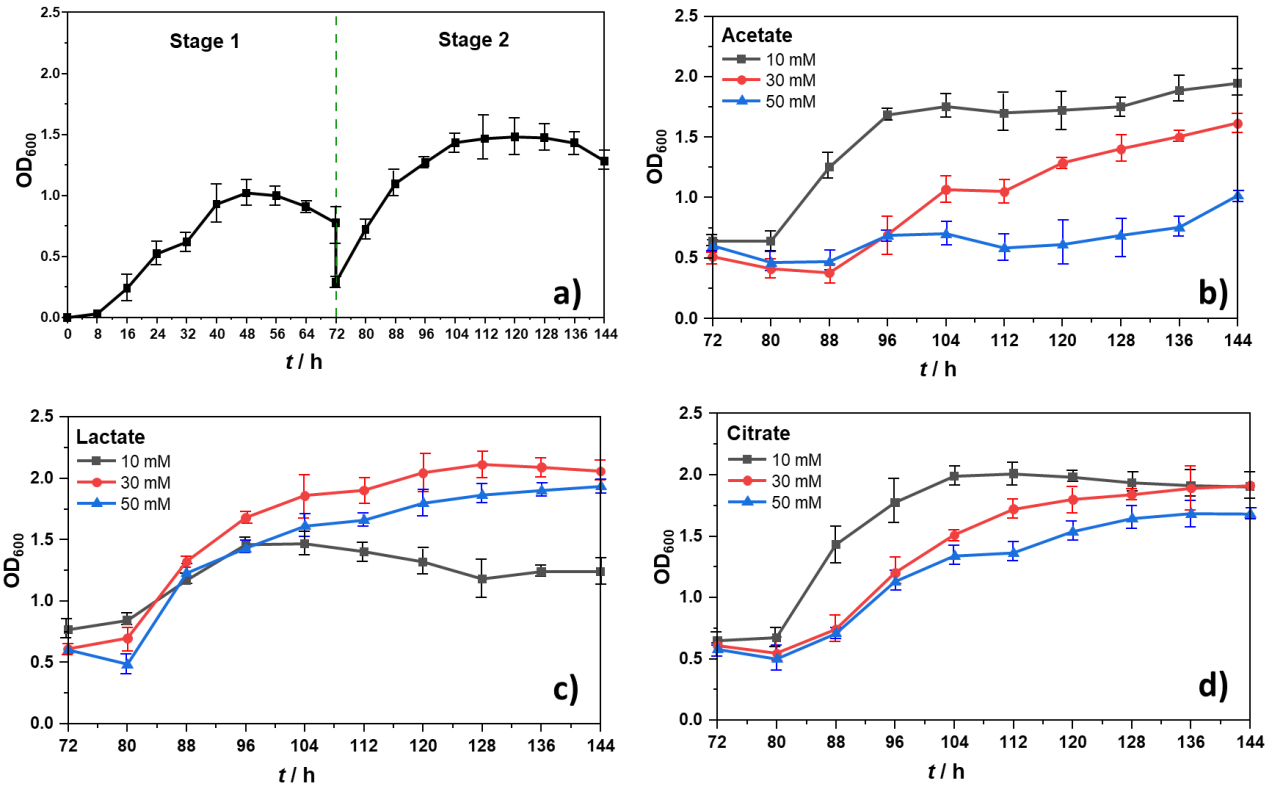

Figure 1. *Two-stage growth and carbon-source response: (a) batch culture in halophilic medium (Stage 1) for 72 h followed by a medium switch at another 72 h initiating Stage 2 at OD_{600}; (b-d) Stage-2 growth in basal medium supplemented with (b) acetate, (c) lactate or (d) citrate at 10 (■), 30 (●) or 50 mM (▲)*

This trend illustrates *B. clausii*'s capacity to sustain metabolic activity despite variations in nutrition availability, a crucial trait for halophilic bacteria in MFC systems. Acetate supplementation

(Figure 1b) yielded better growth at 10 mM (OD_{600} = 1.78±0.01), whereas dosages of 30 to 50 mM reduced growth due to osmotic stress and potential uncoupling effects [16]. Lactate (Figure 1c) exhibited a distinct pattern: best growth was seen at 30 mM (2.23±0.02), suggesting that this intermediate concentration is more congruent with the physiological tolerance of *B. clausii* [17]. In the case of citrate (Figure 1d), higher growth occurred at concentrations of 10 to 30 mM, while a decline was seen at 50 mM, consistent with findings indicating elevated citrate levels may disrupt aerobic respiration and carbon metabolism within the Krebs cycle [18,19].

Nevertheless, elevated OD_{600} did not consistently correlate with MFC performance. Numerous studies indicate that elevated cell density may be offset by a reduction in the proportion of electroactive cells, thereby decreasing electron transfer efficiency [20]. Consequently, the analysis of growth curves must be coupled with the electrochemical response to understand the substrate's role in electrogenic activity, rather than focusing solely on cellular proliferation. At 72 h, most cultures enter the stationary phase, during which metabolic activity and electron production begin to decline [21]. Consequently, 72 hours was selected as the operational endpoint in MFC testing, signifying the culture stage prior to a notable reduction in electrogenic ability.

Half-cell characteristics

Figures 2a to 2i depict voltammograms from cyclic voltammetry analysis before to and after incubation (*t* = 0 and *t* = 72 h) for each modification of carbon source (acetate, lactate, and citrate). The increase in redox peak intensity at 72 hours, shown by the yellow square, corroborates that *Bacillus clausii* J1G-0%B maintained prolonged metabolic activity throughout the incubation period. This action led to increased electron transport and the buildup of electroactive chemicals as the cells proliferated.

The changes in redox peaks for acetate (Figures 2a to 2c) and lactate (Figures 2d-f) between 0 and 72 h were minimal, suggesting that both substrates are rapidly digested, resulting in a consistent electroactive response. Conversely, the citrate variation (Figures 2g to 2i) exhibited a much greater disparity in redox peaks. This suggests that citrate metabolism is more sluggish and intricate, leading to more variability in the kinetics of electron generation and transfer over the incubation period. The structural complexity of citrate, in contrast to acetate and lactate, is recognized to diminish the efficiency of electron generation and transmission by bacillus [22].

The oxidation potentials of acetate and lactate at different concentrations vary from 0.167 to 0.293 V against Ag/AgCl (0.364 to 0.490 V *vs*. SHE), may be associated with terminal oxidase-related cytochromes (*e.g*. a_3 or b) redox reaction: cytochrome a_3 (Fe^{3+}) + e^- → cytochrome a_3 (Fe^{2+}). The maximum oxidation potential of citrate is 0.321 to 0.366 V relative to Ag/AgCl (0.518 to 0.563 V *vs.* SHE), remaining within the same redox range but exhibiting a greater peak amplitude, indicative of the extended dynamics of citrate metabolism. The reduction potential of 10 mM acetate and lactate ranged from 0.037 to 0.054 V relative to Ag/AgCl (0.234 to 0.251 V *vs.* SHE), consistent with redox-active heme-containing proteins reported for bacterial respiratory chains, such as cytochrome c/c_1 redox reaction: cytochrome c_1 (Fe^{3+}) + e^- → cytochrome c_1 (Fe^{2+}). At lactate and citrate concentrations of 30-50 mM, the reduction potential rose to 0.059 to 0.087 V relative to Ag/AgCl (0.256 to 0.284 V *vs.* SHE), indicating the participation of cytochrome c_1. Simultaneously, 10 mM citrate exhibited a reduction potential of −0.074 V relative to Ag/AgCl (0.123 V *vs.* SHE), indicating a cytochrome b redox reaction: cytochrome b (Fe^{3+}) + e^- → cytochrome b (Fe^{2+}).

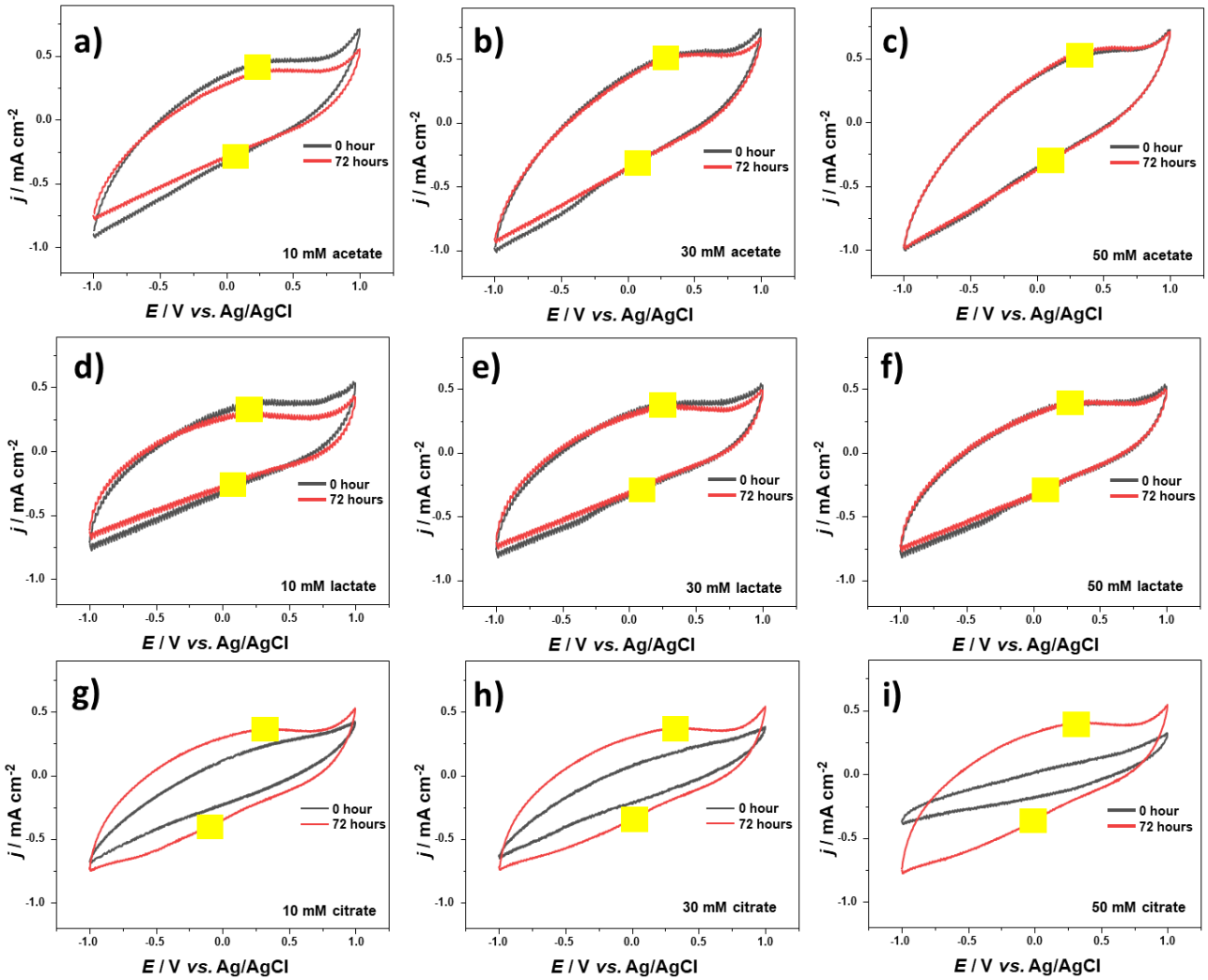

Figure 2. *Cyclic voltammetry of halophilic MFCs before and after Stage-2 incubation with carboxylates. Panels are labelled as in the figure: (a-c) acetate at 10, 30 and 50 mM; (d-f) lactate at 10, 30 and 50 mM; (g-i) citrate at 10, 30 and 50 mM, all at scan rate 100 mV s^{-1}. Black traces are the raw forward/reverse sweeps before incubation; the red trace is the CV after Stage-2 incubation in the indicated carboxylate; yellow squares mark anodic and cathodic peak positions*

The redox profiles across different carbon sources exhibited a uniform pattern, consistent with other results. Modestra and Mohan [23] documented the standard redox potentials of *Bacillus spp.* as 0.237 V (cytochrome c), 0.408 V (cytochrome c_1), and 0.620 V (cytochrome a_3) relative to the standard hydrogen electrode (SHE). Research conducted by Christwardana *et al*. [7,8] demonstrated a broader range, from -0.460 to 0.317 V *vs*. SHE, substantiating the participation of cytochrome b to cytochrome a. Minor discrepancies across investigations are likely attributable to changes in pH, metabolite accumulation, electroactive cell density, and adsorption processes on the electrode surface [24]. The variations and magnitudes of the redox peaks in this research not only indicate the distinct metabolic pathways of each substrate but also demonstrate the influence of biochemical variables in the electrode microenvironment on microbial electron transfer.

Cyclic voltammetry investigations at diverse scan rates (0.1 to 1.6 V s^{-1}) demonstrated an increase in peak current with increasing scan rate. This response illustrates the MFC system's sensitivity to potential changes, and the resulting voltammograms were subsequently used for further analysis, including characterization of the rate-determining step (RDS) and determination of the electron transfer rate constant (k_s) [7].

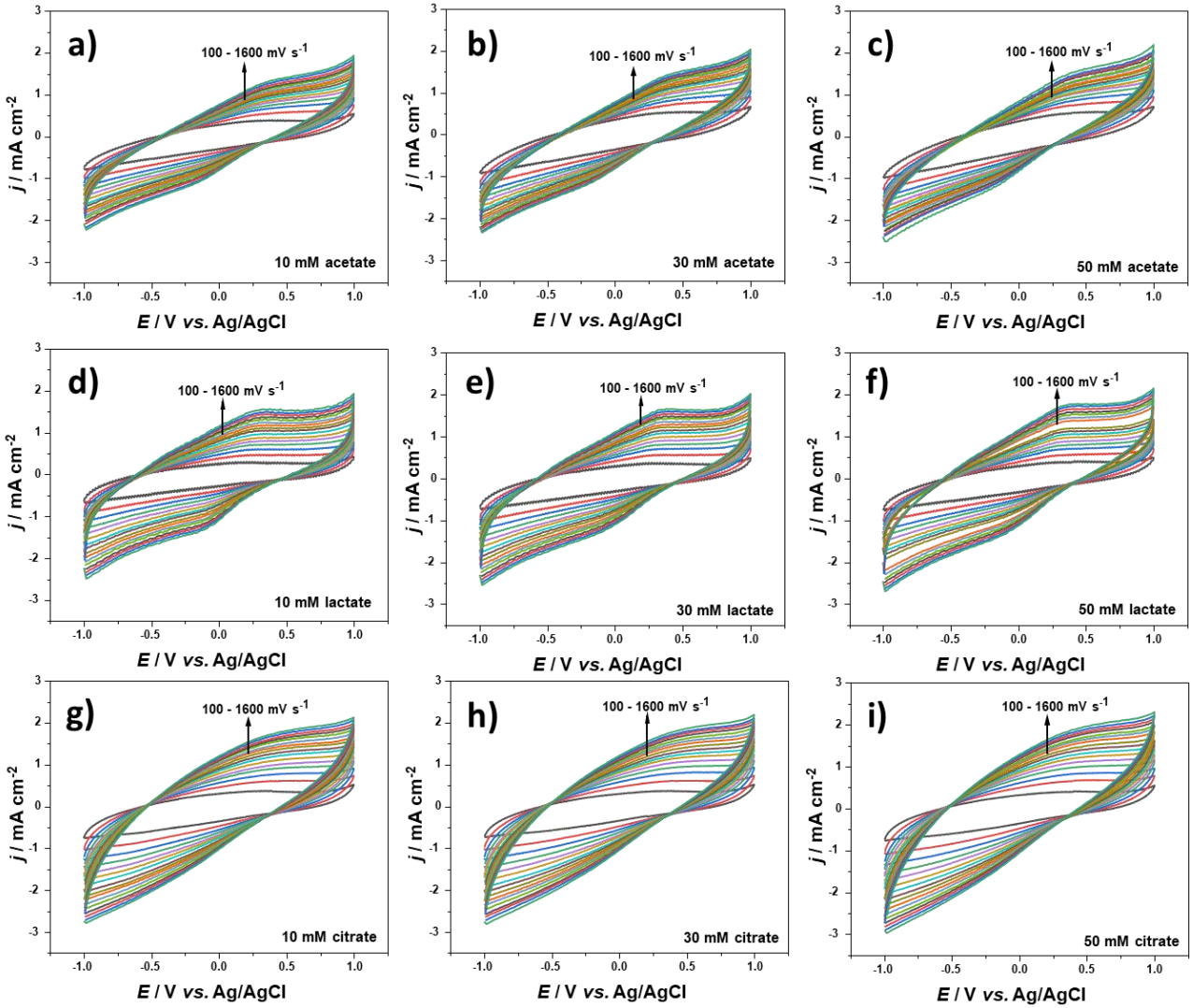

Figure 3. *Cyclic voltammograms (CVs) of halophilic MFC anodes after Stage-2 incubation under various scan rates. Panels are labelled as in the figure: (a-c) acetate at 10, 30 and 50 mM; (d-f) lactate at 10, 30, 50 mM; (g-i) citrate at 10, 30 and 50 mM. Within each panel, the coloured traces are CVs recorded at scan rates 100 to 1600 mV* s^{-1}

The alterations in the redox peaks corresponding to each scan rate change (Figure 3a to 3i) demonstrate the hallmark features of a quasi-reversible system. Augmenting the scan rate intensifies the overpotential effect, which arises when electron transport lags behind the acceleration of the applied potential. Under these circumstances, the system requires a higher oxidation potential and a more negative reduction potential to sustain the redox process, leading to a greater peak shift at higher scan rates [25].

With increasing overpotential, the voltammogram becomes more asymmetric, and the peak potential difference exceeds the theoretical value of 57 mV for a reversible one-electron process. This signifies that at higher scan rates; the redox process is progressively influenced by kinetic constraints and ceases to exhibit perfect reversible conditions. As a result, the correlation between peak current and the square root of scan rate ceases to be linear, rendering the Randles-Ševčik equation unsuitable for analysing the system under these circumstances. The existence of overpotential does not inherently indicate that the reaction is irreversible. The extent of reversibility may be assessed by the ratio of the peak oxidation current to the reduction current (I_{pa}/I_{pc}). The electrochemical response in this system is quasi-reversible, with biofilm growth and diffusion constraints affecting it [26].

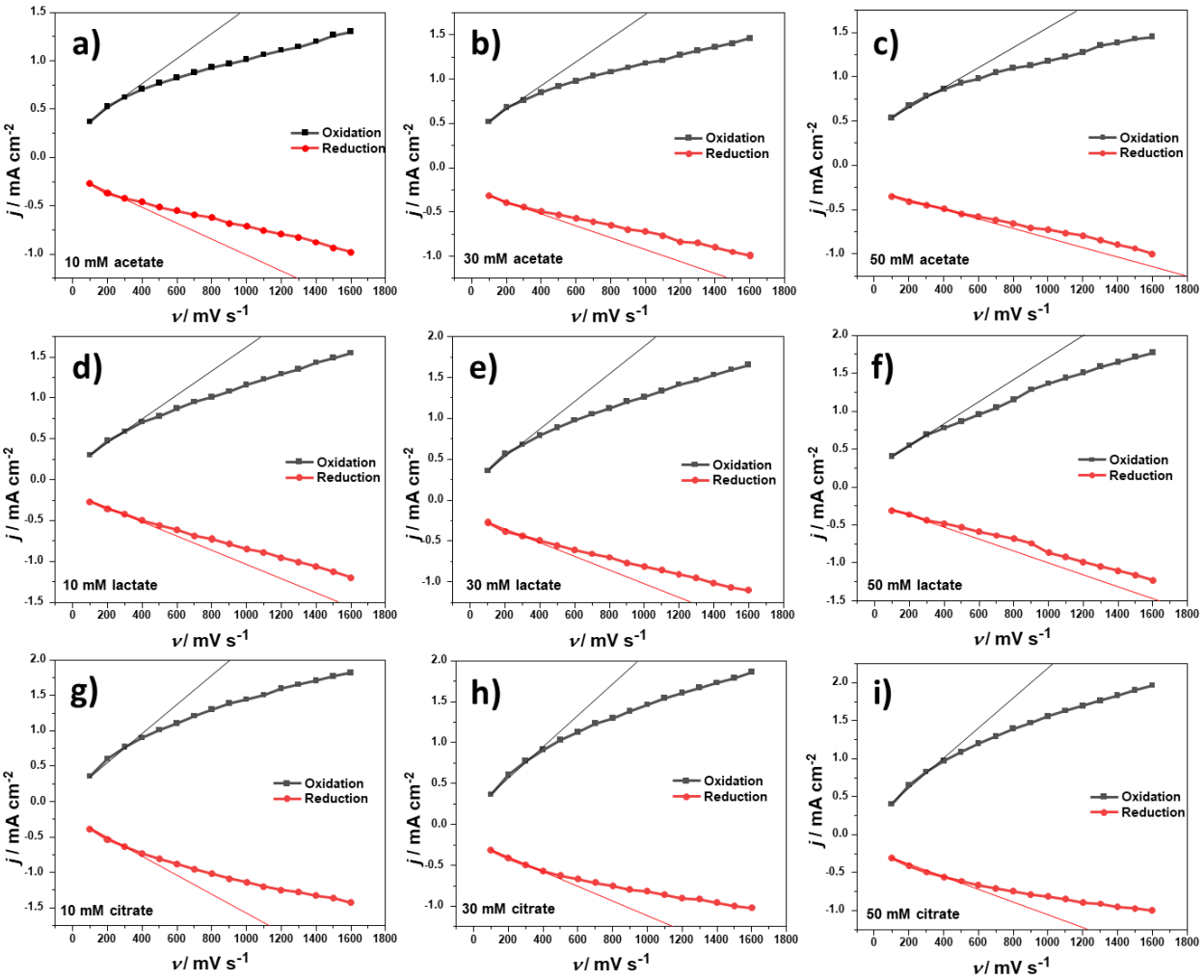

Figure 4. *Scan rate dependence of peak current density to diagnose the rate-determining step in halophilic MFC anodes after Stage-2 incubation. Panels are labelled as in the figure: (a-c) acetate at 10, 30 and 50 mM; (d-f) lactate at 10, 30 and 50 mM; (g-i) citrate at 10, 30, 50 mM*

Rate-determining step (RDS) analysis demonstrated that all changes in carbon sources showed a nonlinear peak-current-scan rate correlation (Figure 4a to 4i), indicating that the redox process at the bacteria-electrode interface is governed by a diffusion-limited mechanism. This indicates that the electron transfer rate is not exclusively controlled by the applied voltage but rather depends on the diffusion of endogenous mediators or cytochrome species to the electrode surface before the reaction occurs [27]. The diffusion constraint significantly constrains current output in MFC systems. Compared with citrate, the RDS patterns for the acetate and lactate variants showed a greater propensity for linearity, indicating enhanced electron-transfer kinetics. This aligns with the more straightforward and compatible metabolic roles of acetate and lactate in the *B. clausii* respiratory pathway, hence reducing diffusion barriers during substrate oxidation. Citrate showed the most pronounced deviation from linearity, indicating a markedly diffusion-limited mechanism. Consequently, acetate and lactate provide superior kinetic conditions for the electrochemical performance of MFCs compared to citrate.

The investigation of k_s was conducted using Laviron's [12] methodology to clarify the electron transfer mechanism and electrochemical characteristics of the MFC system. A high k_s value signifies accelerated electron transport between *B. clausii* J1G-0%B cells and the electrode, hence immediately enhancing the maximum voltage and power density attained by the MFC [7,12,21].

Consequently, k_s served as the principal metric for comparing the control system with systems supplemented with carbon in the form of acetate, lactate, or citrate.

The calculations indicated that 50 mM acetate supply yielded the greatest k_s, measuring 1.888±0.002 s^{-1}, followed by 50 mM lactate and intermediate concentrations of acetate and lactate (Figure 5a to 5i). The addition of all carbon sources enhanced k_s by 184.56 to 378.23 % relative to the control (0.395±0.001 s^{-1}), therefore indicating that carboxylate supplementation significantly increased the electron transfer capacity of *B. clausii* at the anode. This augmentation aligns with the enhanced availability of electrons from the catabolic routes of acetate, lactate, and citrate [9].

Acetate demonstrated enhanced electrochemical performance owing to its direct conversion to acetyl-CoA, which effectively integrates into the Krebs cycle, facilitating the production of more stable endogenous reductants and mediators [22]. Lactate exhibited the same pattern, necessitating first conversion to pyruvate before to accessing the identical route [4]. Conversely, citrate demonstrated the lowest k_s value at elevated concentrations (50 mM), suggesting constraints in citrate metabolism by *B. clausii* and possible disturbances in cellular homeostasis, encompassing osmotic stress and diminished enzymatic activity related to respiration [4,22]. These circumstances increase electron-transfer resistance and diminish redox efficiency. Acetate offers the most straightforward and efficient metabolic route for facilitating electron transport, followed by lactate, while citrate presents metabolic constraints that hinder k_s attainment at elevated concentrations.

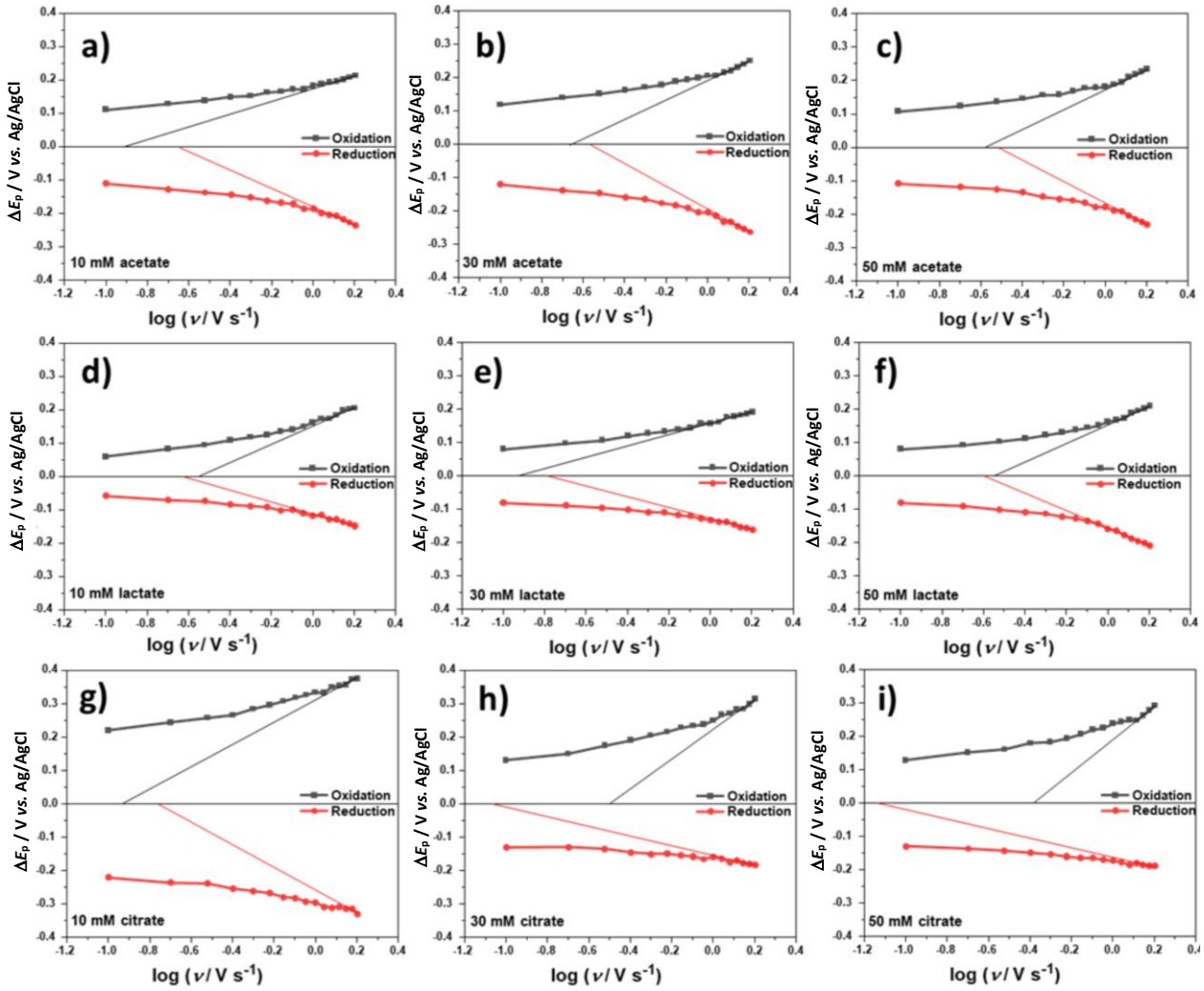

Figure 5. *Laviron plot of halophilic MFC bioanodes after Stage-2 incubation. Panels are labelled as in the figure: (a-c) acetate at 10, 30 and 50 mM; (d-f) lactate at 10, 30 and 50 mM; (g-i) citrate at 10, 30 and 50 mM*

pH is a critical factor in evaluating the metabolic stability and electrochemical efficacy of microorganisms in microbial fuel cells (MFCs). Alongside electron production, halophilic bacteria generate organic acids, ammonia, and various metabolites that can alter the medium's pH during incubation [28,29]. The pH fluctuations recorded for each carbon source are illustrated in Figures 6a to 6c.

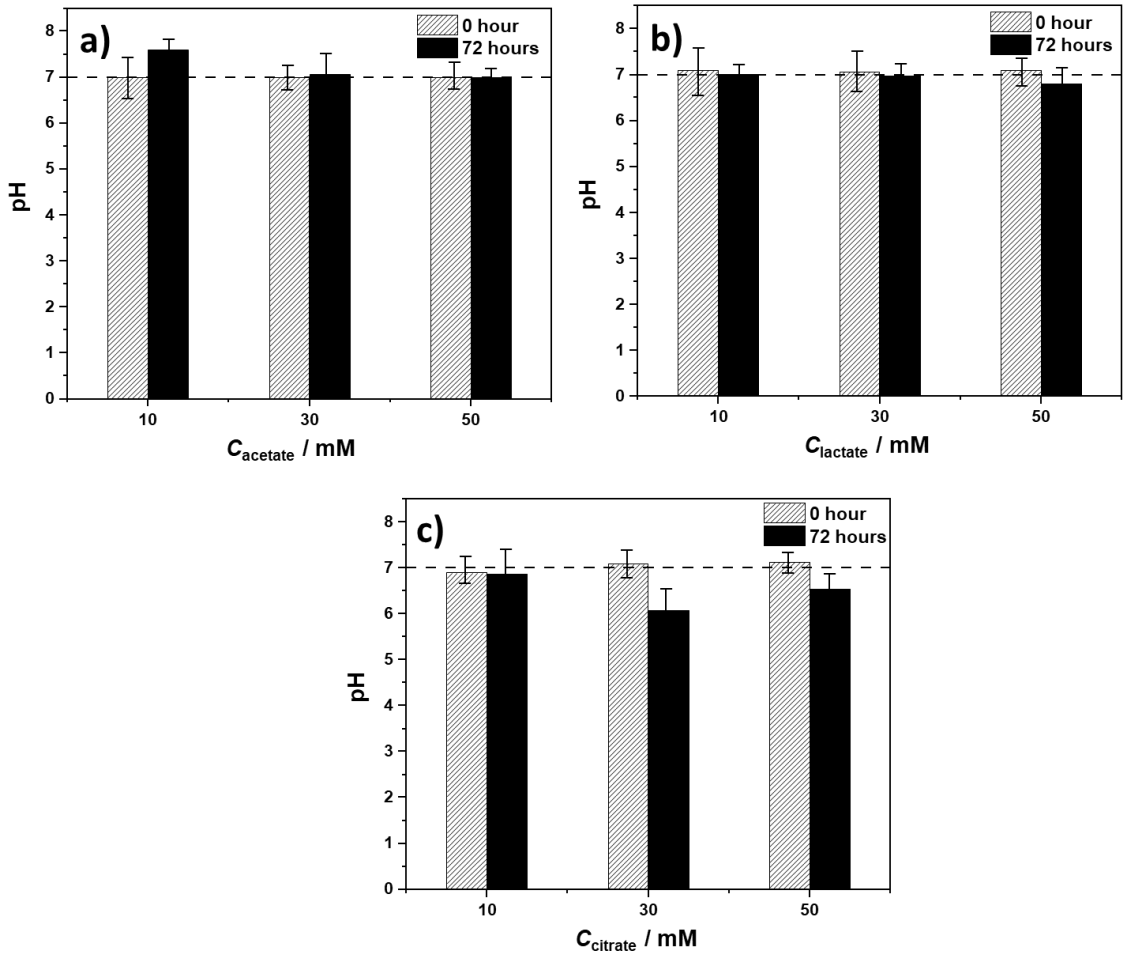

Figure 6. *pH of halophilic MFC anolytes before and after Stage-2 incubation with various carboxylates: (a) acetate at 10, 30 and 50 mM; (b) lactate at 10, 30 and 50 mM; (c) citrate at 10, 30 and 50 mM*

The use of acetate elevated pH throughout incubation, whereas lactate and citrate reduced it. This signifies variations in catabolic pathways: acetate metabolism by *B. clausii* J1G-0 %B yields more alkaline metabolites, whereas lactate and citrate catabolism generate more acidic metabolites. The lowering trend in pH becomes more pronounced at higher substrate concentrations, suggesting that increased carboxylate availability increases the metabolic burden and organic acid production [28]. The pH range (6.08 to 7.59) was close to neutrality, aligning with the ideal growth range for *Bacillus spp*. [30], so demonstrating that the culture remained physiologically active.

Ammonia serves as an indication of nitrogen metabolism from tryptone/yeast extract and to monitor possible buildup that may influence the pH established during incubation. Ammonia is produced by the deamination of amino acids derived from the nitrogen source (tryptone), and its presence serves as an indirect indicator of bacterial metabolic activity associated with electron transfer [29]. Acetate variations yielded the greatest ammonia concentrations (0.35 to 0.75 ppm), followed by lactate (about 0.25 ppm) and citrate (0.20 to 0.25 ppm). This trend aligns with prior electrochemical findings, suggesting that acetate metabolism induces the most physiological activity

and metabolite synthesis, followed by lactate and citrate. Overall, our data demonstrate that the pH response and ammonia generation are linked with the metabolic activity levels of *B. clausii* J1G-0%B towards each carbon source.

Full-cell characteristics

The voltage difference between the anode and cathode indicates the quantity of electrochemical energy obtainable from bacterial metabolism in the MFC circuit [21]. Figures 7a-7c illustrate the voltages produced during three cycles of fed-batch operation, each lasting 72 hours.

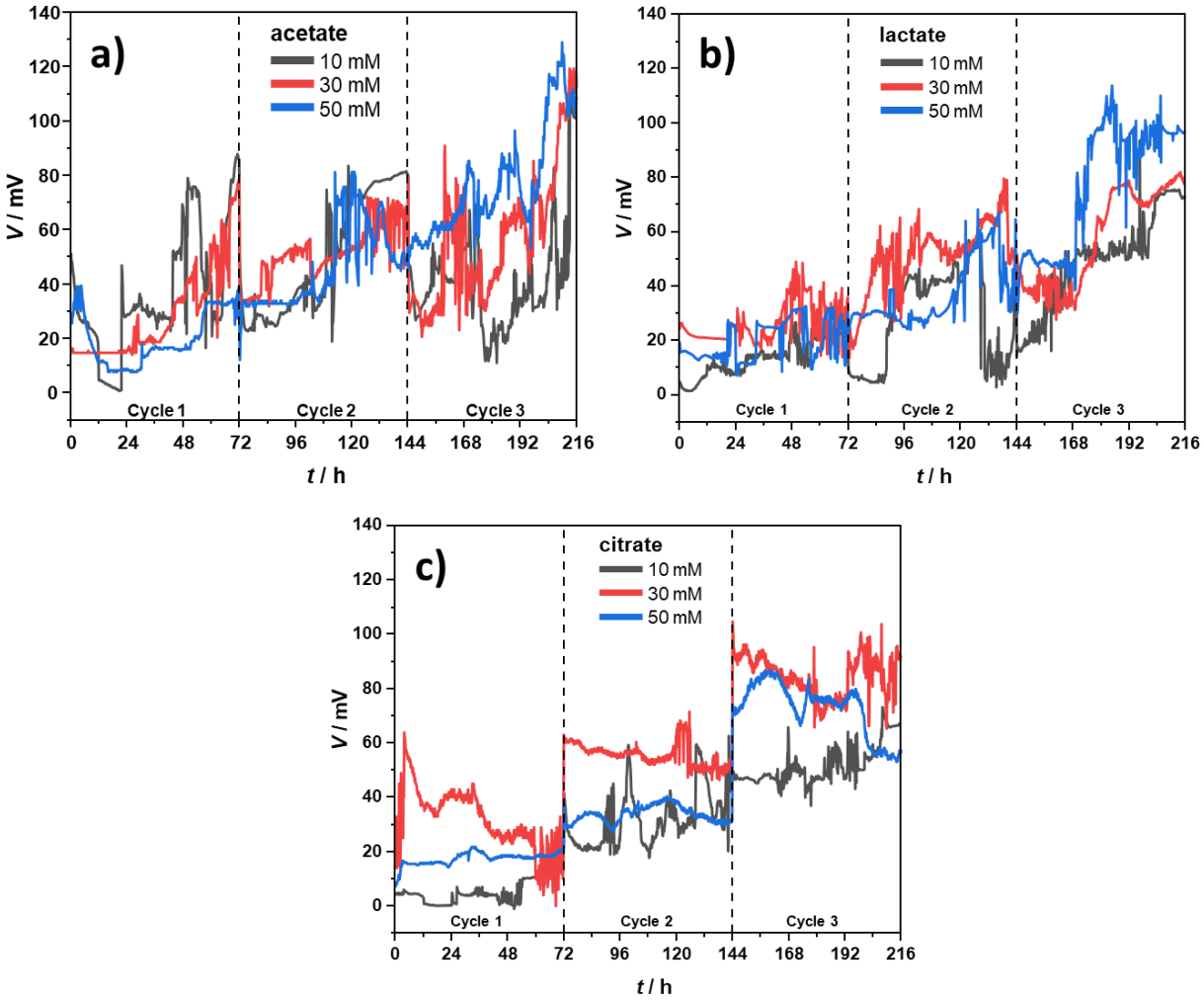

Figure 7. *Cell voltage-time profiles of halophilic MFCs during Stage-2 incubation with various carboxylates: (a) acetate, (b) lactate, (c) citrate*

In the case of the acetate and lactate substrates (Figure 7a to 7b), *B. clausii* J1G-0%B demonstrated a characteristic pattern of an adapting system: the starting voltage at hour 0 was minimal, then rose steadily until the conclusion of the first cycle at hour 72. This pattern recurred in the second and third rounds, with the starting voltage remaining low while escalating more quickly in subsequent cycles. This augmentation signifies the development of the anode biofilm and enhanced electron-transfer efficiency as electrogenic consortia form on the electrode surface.

Conversely, with citrate (Figure 7c), the initial voltage at hour 0 exceeded that of the other two substrates. The voltage thereafter diminished or steadied until the conclusion of each cycle. This pattern was uniform over all three observed cycles. The elevated initial voltage in citrate is believed to stem from transient capacitive charging, attributed to its three carboxylate groups that enhance

double-layer capacitance and promote temporary charge buildup at the electrode interface [10,31]. This capacitive effect is temporary and dissipates after the charge is discharged during MFC operation.

The mean voltage escalated with each cycle across all substrate categories. The decreased voltage in the first cycle indicates a physiological adaptation period and the absence of stable biofilm formation. In the second cycle, the elevated voltage indicates increased metabolic activity and enhanced electron transfer within the biofilm. The apex transpired during the third cycle, characterized by a substantial rise in voltage as a mature biofilm developed and electron transport channels became more efficient [32]. This pattern aligns with the kinetics of electrogenic biofilm formation often seen in MFC systems.

The greatest average voltage recorded was 77.87 mV at 50 mM acetate, followed by 65.61 mV at 50 mM lactate and 59.48 mV at 30 mM citrate. The findings demonstrate that acetate is the most effective substrate for *B. clausii* J1G-0%B in producing electrogenic activity. This aligns with prior electrochemical research indicating the peak k_s value at 50 mM acetate [22]. Biochemically, acetate has the most straightforward metabolic route, immediately entering the TCA cycle via acetyl-CoA, hence facilitating a more steady and efficient electron flow. Lactate and citrate need supplementary oxidation processes, which impede electron transport and diminish average voltage performance. The observations confirm that the presence of metabolically suitable substrates is essential in influencing the electrogenic capacity of halophilic bacillus-based MFCs and highlight the significance of mature biofilms as a crucial component in MFC performance.

The study of maximum power density (MPD) was used to determine the ideal operating point at which the MFC generates peak power output. This measure delineates the correlation between voltage and current across different external loads, hence indicating the system's internal resistance, energy conversion efficiency, and the stability of the electrochemical process throughout operation [21]. Figures 8a to 8c illustrate the MPD findings for each change in carbon substrate.

The acetate and lactate variants had the highest MPD at 50 mM, followed by 30 and 10 mM. This trend demonstrates that elevated substrate concentration enhances the availability of electrons from bacterial catabolism, thereby augmenting power density [9]. Nonetheless, this impact does not remain linear forever. The higher MPD value for the citrate substrate was attained at 30 mM, but 50 mM yielded worse performance. This occurrence indicates a physiological tolerance threshold for citrate, which, at elevated concentrations, may disrupt cellular homeostasis and induce osmotic stress, thereby diminishing electron flow and electrochemical efficiency [33]. Moreover, citrate metabolism is more complex and requires additional pathways before entering the TCA cycle, thereby reducing the electron transfer rate relative to acetate and lactate.

The maximum power density was quantitatively greatest at 58.16±3.54 mW m^{-2} for 50 mM acetate, followed by 38.36±4.25 mW m^{-2} for 50 mM lactate and 26.88±3.86 mW m^{-2} for 30 mM citrate. The use of 50 mM acetate yielded relatively high performance due to its simple molecular structure, which facilitates rapid conversion to acetyl-CoA, thereby producing a steady NADH/$FADH_2$ flux and enhancing electron transfer to the anode [22]. The alignment of these findings with earlier half-cell studies, which similarly exhibited optimal electrochemical performance at 50 mM acetate, substantiates that acetate is the most suitable substrate for *B. clausii* J1G-0%B metabolism and the most efficacious in facilitating electrogenic biofilm development.

Nonetheless, 50 mM lactate and 30 mM citrate generated substantial MPD and have the potential to serve as alternate substrates in halophilic *Bacillus*-based MFC systems. This illustrates the metabolic versatility of *B. clausii* J1G-0%B, albeit the peak electrogenic efficiency was attained on acetate.

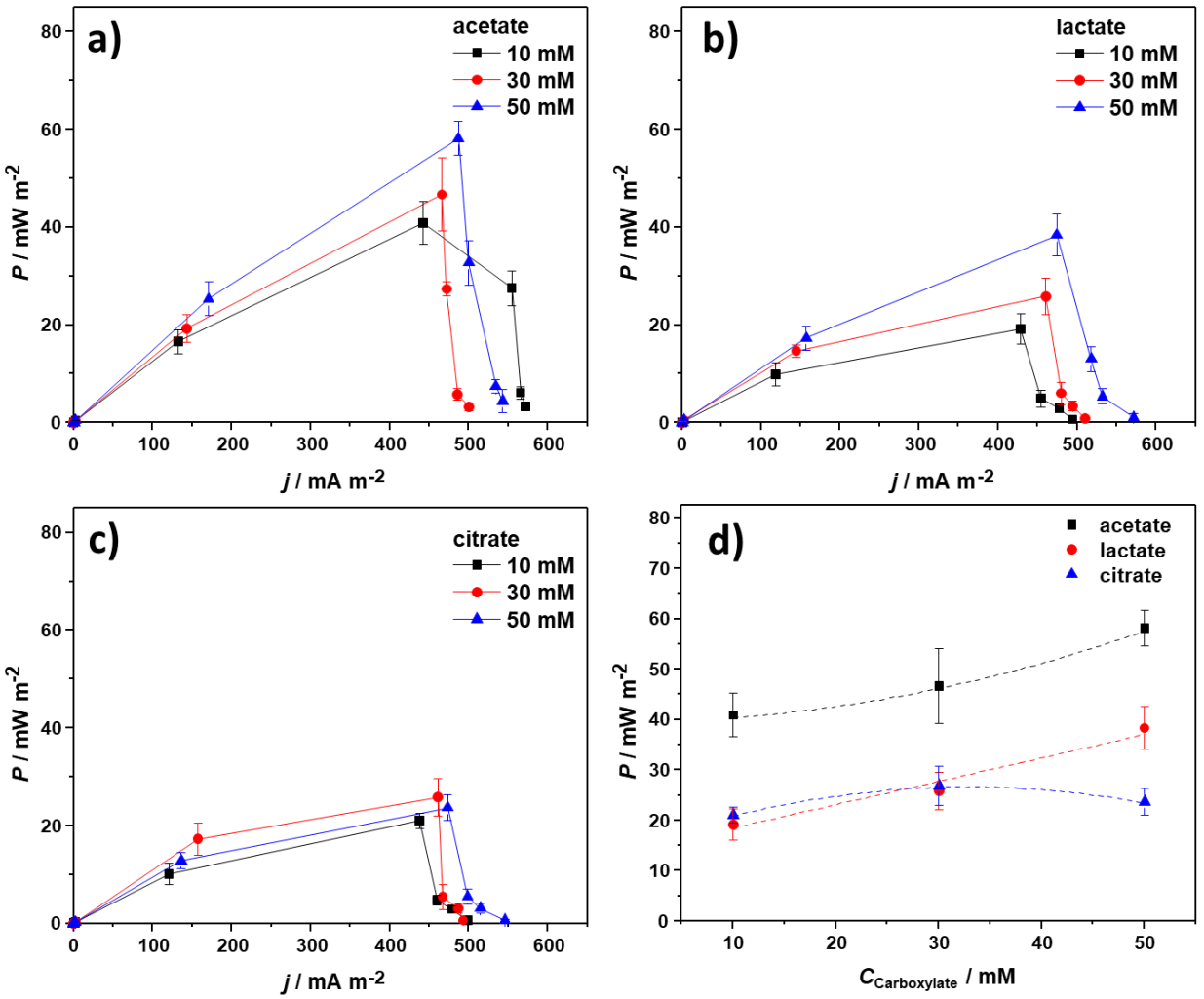

Figure 8. *Power-current characteristics of halophilic MFCs during Stage-2 incubation with various carboxylates: (a) acetate, (b) lactate, (c) citrate and (d) maximum power density as a function of substrate concentration for carboxylate in a* Bacillus clausii *J1G-0%B-based MFCs*

The MPD achieved in this work (58.16 mW m^{-2}) is inferior to other reports of consortium-based halophilic MFCs functioning at salinities of 20 to 70 g L^{-1} (162-570 mW m^{-2}). This investigation was conducted under hypersaline conditions of 100 g L^{-1} NaCl (about 10 %), which is considerably greater than most other reports, as shown in Table 1 [2,5,34-38]. At this salinity level, high osmotic pressure requires microorganisms to expend metabolic energy to maintain cellular homeostasis, potentially reducing the proportion of electrons available for EET. Beyond salinity, most research on elevated MPDs uses microbial consortia and platinum or Pt/C-based cathodes, known for their exceptional catalytic activity in oxygen reduction. This research employed a pure culture of *Bacillus clausii* J1G-0%B and a carbon electrode, omitting the use of specialized catalytic materials like platinum on the cathode. This disparity directly influences the kinetics of the cathodic reaction and the internal resistance of the system, resulting in an elevated MPD value. Nonetheless, compared with a previously documented single-culture *Bacillus circulans* BBL03-based MFC (17.42 mW m^{-2}), this system exhibits a notable enhancement in power output, even at elevated salt levels. The primary contribution of this study is the demonstration of electron transfer viability under extreme hypersaline conditions using pure cultures, providing a more controlled mechanistic foundation for understanding EET regulation under elevated osmotic pressure.

Table 1. *Comparative analysis of halophilic MFC performance under varying operating conditions*

Anode	Cathode	Microbes	Reactor type	Salinity, g L^{-1}	Maximum power density, mW m^{-2}	Ref.
Carbon felt	Carbon felt	Halophilic exo-electrogenic consortium bacteria	Dual chamber	40	162.09	[5]
Carbon brush	Pt coated carbon cloth	Halophilic consortium bacteria	Single chamber	37.7	165	[34]
Carbon brush	Pt crystal coated carbon cloth	Halophilic consortium bacteria	Single chamber	69.5	570	[35]
Stainless steel mesh	Graphite felt	Halophilic consortium bacteria	Double chamber	58.44 (1 M NaCl)	207.05	[36]
Carbon brush	Pt crystal coated carbon cloth	Halophilic consortium bacteria	Single chamber	46	420	[2]
Carbon felt	Pt/C coated carbon cloth	Halophilic electroacti-ve consortium bacteria	Double chamber	20	276	[37]
Carbon felt	Pt-coated carbon	*Bacillus circulans* BBL03	Double chamber	-	17.42	[38]
Carbon felt	Carbon felt	*Bacillus clausii* J1G-0%B	Single Chamber	100	58.16	This work

Figure 8d shows the relationship between substrate concentration and maximum power density (MPD for three carboxylates: acetate (black curve), lactate (red curve), and citrate (blue curve). Each curve exhibits a nonlinear response, reflecting the interrelationships among substrate availability, microbial metabolism, and electron-transfer efficiency at the anode. The acetate curve shows a nearly monotonic increase in MPD with increasing concentration, reaching a peak value at 50 mM. This trend indicates that acetate can be efficiently metabolized by *Bacillus clausii* J1G-0%B via direct conversion to acetyl-CoA, thereby providing a stable, continuous supply of electrons for extracellular electron transfer processes. The absence of a decrease in MPD at high concentrations indicates good physiological tolerance to acetate across the tested concentration range. In contrast, the lactate curve shows a moderate increase in MPD with concentration, but with a gentler slope than that of acetate. This suggests that although lactate can function as an electron donor, the need for initial conversion to pyruvate before entering the TCA cycle limits the rate of electron generation and the efficiency of energy conversion at higher concentrations. The citrate curve exhibits a bell-shaped behaviour, with maximum MPD reached at intermediate concentrations, then decreasing at higher concentrations. This pattern indicates metabolic and physiological limits to citrate utilization, possibly related to the complexity of the metabolic pathway, osmotic imbalance, or disruption of cellular homeostasis at high concentrations. The decrease in MPD at high citrate concentrations confirms that increased substrate availability does not necessarily translate to improved electrochemical performance. The differences in curve shapes confirm that the type of substrate and its metabolic route directly control the maximum power density, with acetate being the most effective substrate, followed by lactate, while citrate shows limitations at high concentrations.

The biofilm mass on the anode reflects the density and distribution of *B. clausii* J1G-0 % B cells, which are essential for electron transfer and energy production in MFC systems. Effectively structured biofilms are not always the thickest; instead, they exhibit elevated electrochemical activity and decreased diffusion resistance [34]. Consequently, biofilm mass serves as a metric for the durability and enduring stability of bacterial electrogenic activity [21].

Following washing to remove salt, the dry biofilm mass varied with the type and concentration of carbon. It is seen from Figure 9 that 50 mM biofilm exhibited a mass of 0.36±0.06 g in acetate, which was smaller than the 10 mM biofilm mass of 0.92±0.05 g, however produced substantially

more power. This suggests that high concentrations of acetate promote the development of thinner yet more electroactive biofilms, aligning with existing research on thin, high-conductivity biofilms associated with Bacillus-based anodes [39].

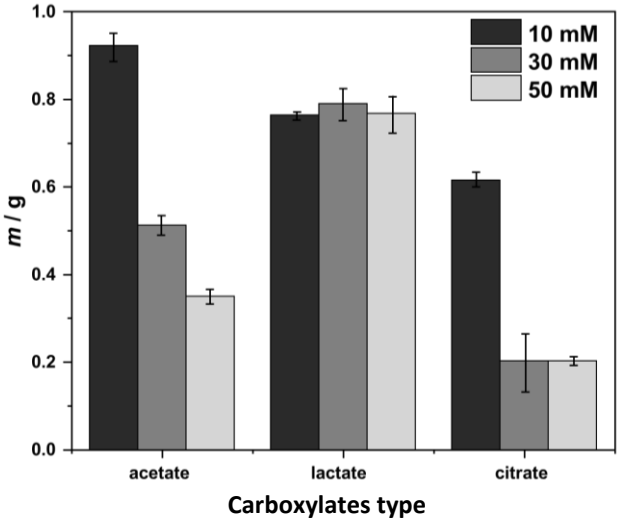

Figure 9. *Biofilm mass on MFC anodes after Stage-2 incubation with carboxylates. Final biofilm mass harvested from anodes following Stage-2 incubation in acetate, lactate, or citrate at 10 mM, 30 mM and 50 mM*

The biofilm mass with lactate remained largely unchanged over the concentration range (0.77 to 0.79 g), suggesting that lactate did not substantially influence biomass growth. The improvement in electrical performance at higher concentrations is likely attributable to improved electron-transfer efficiency rather than to increased biofilm thickness. The established biofilm is metabolically active, although there is no mass gain. Conversely, with citrate, biofilm mass decreased significantly from 0.65±0.02 g (10 mM) to 0.20±0.03 g at 30 and 50 mM. This reduction was followed by an increase in power density, indicating an inverse link between biofilm thickness and cellular function. The direct incorporation of citrate into the TCA cycle may enhance electron generation, even under reduced biomass, resulting in a sparse biofilm with elevated electrochemical activity. The reduction in mass may be linked to ionic stress or the buildup of organic compounds that impede cell growth [39].

Results in Figure 9 indicate that the enhancement in MFC performance after the incorporation of a carbon substrate is attributable not to an increase in biofilm bulk, but to an improvement in the electrochemical quality of the biofilm. Thinner and more porous biofilms exhibit enhanced substrate diffusivity, reduced internal resistance, and increased electron conductivity, leading to more efficient charge transfer [21,39]. Consequently, biofilm mass is not the only determinant of MFC performance; rather, electrochemical parameters are much more critical in assessing *B. clausii* J1G-0%B-based systems.

Nexus between electron transfer kinetics, power density, and biofilm characteristics

The relationship between the k_s, MPD, and biofilm mass indicates that the performance of the *Bacillus clausii* J1G-0%B-based MFC is determined more by the electrochemical efficiency of the biofilm than the amount of biomass alone. Increasing k_s was consistently accompanied by an increase in MPD, particularly in the 50 mM acetate treatment, reflecting that accelerated electron transfer at the biofilm-electrode interface directly increases the system's power generation capacity (Figure 10a). Conversely, biofilm mass showed a more negative correlation with either k_s or MPD, as shown in Figure 10b. Under 50 mM acetate conditions, relatively thinner biofilms produced the higher k_s and MPD values, indicating that thin, yet highly electroactive biofilms are more advantageous than thick biofilms, which potentially suffer from substrate diffusion limitations and increased

internal resistance. This phenomenon confirms that increasing electrogenic activity per unit biomass is more important than quantitative cell accumulation. For lactate and citrate substrates, a similar pattern was observed, where the increase in MPD was more related to k_s than to biofilm growth. These results indicate that k_s serves as the primary linking parameter between microbial metabolism and MFC power performance, while biofilm mass plays a secondary role and cannot be used as a sole indicator of system performance.

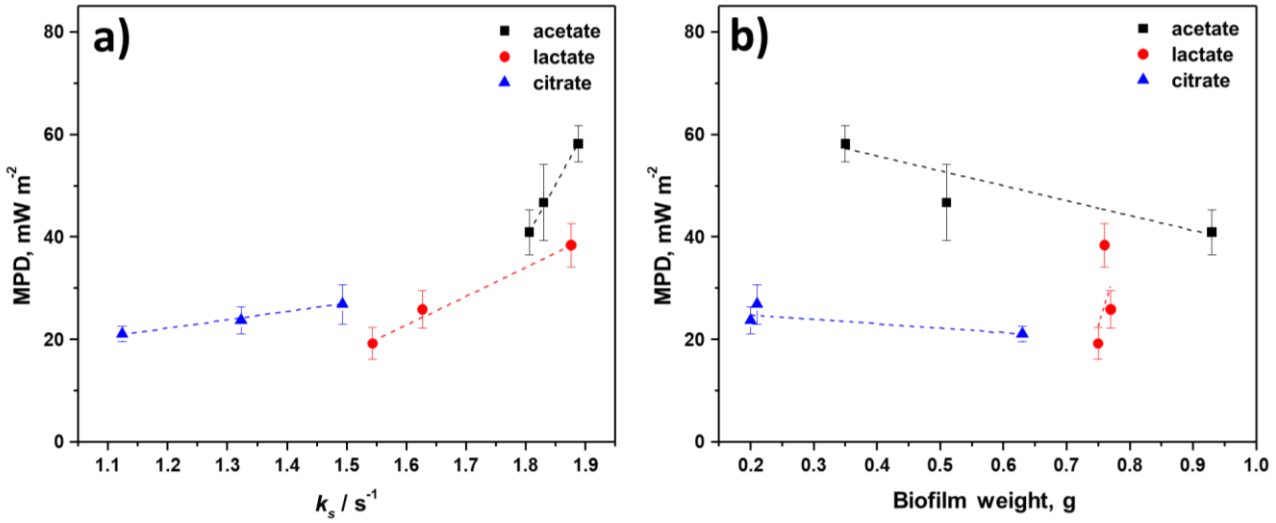

***Figure 10**. Correlation between maximum power density (MPD) and (a) electron transfer rate constant (k_s), (b) biofilm weight in Bacillus clausii J1G-0%B-based MFC anodes*

Conclusions

This study revealed that the addition of acetate, lactate and citrate significantly enhanced the electrochemical performance of a microbial fuel cell (MFC) system using the halophilic bacteria *Bacillus clausii* J1G-0%B. At all evaluated concentrations (10, 30, and 50 mM), the incorporation of carboxylates led to marked enhancements in electron transfer characteristics, evidenced by increases in the heterogeneous electron transfer rate constant (k_s), average voltage, and maximum power density relative to the control without additional carbon source. The k_s values rose by 184.56 to 378.23 % compared to the control (0.395±0.001 s^{-1}), with the maximum k_s seen in the 50 mM acetate treatment (1.888±0.002 s^{-1}). Comprehensive cell analysis verified the superior performance of these conditions, achieving an average voltage of 486.94 mV and a peak power density of 58.16±3.54 mW m^{-2}. In comparison, operation with 50 mM lactate produced a lower average voltage of 474.05 mV and a maximum power density of 38.36±4.25 mW m^{-2}, while 30 mM citrate resulted in 460.54 mV and 26.88±3.86 mW m^{-2}. The mass of biofilm did not exhibit a linear correlation with electrochemical performance, suggesting that thin but electroactive biofilms facilitated superior electron transfer efficiency compared to thicker biofilms. The advantage of acetate stems mostly from its straightforward metabolic pathway and its compatibility with the Krebs cycle, thereby facilitating more efficient electron generation than lactate and citrate. These data affirm that supplementation with simple carboxylates, particularly 50 mM acetate, significantly enhances the performance of halophilic MFCs. The findings establish *B. clausii* J1G-0%B as a viable bioelectrocatalyst for hypersaline wastewater treatment, while producing sustainable electrical energy.

***Funding:** This research received no specific grant or financial support from any funding agency in the public, commercial, or not-for-profit sectors.*

***Conflict of interest:** The authors declare that there is no conflict of interest regarding the publication of this article.*

References

[1] Y. C. Ching, G. Redzwan, Biological treatment of fish processing saline wastewater for reuse as liquid fertilizer, *Sustain*ability **9** (2017) 1062. https://doi.org/10.3390/su9071062

[2] M. T. Jamal, A. Pugazhendi, Treatment of fish market wastewater and energy production using halophiles in air cathode microbial fuel cell, *Journal of Environmental Management* **292** (2021) 112752. https://doi.org/10.1016/j.jenvman.2021.112752

[3] A. Castellano-Hinojosa, M. J. Gallardo-Altamirano, C. Pozo, A. González-Martínez, J. González-López, Inoculum selection and hydraulic retention time impacts in a microbial fuel cell treating saline wastewater, *Applied Microbiology and Biotechnology* **109** (2025) 29. https://doi.org/10.1007/s00253-024-13377-y

[4] J. Zhang, Z. Chen, C. Liu, J. Li, X. An, D. Wu, X. Sun, B. Zhang, L. Fu, F. Li, H. Song, Construction of an Acetate Metabolic Pathway to Enhance Electron Generation of Engineered *Shewanella oneidensis, Frontiers in Bioengineering and Biotechnology* **9** (2021). https://doi.org/10.3389/fbioe.2021.757953

[5] A. Vijay, P.C . Ghosh, S. Mukherji, Power Generation by Halophilic Bacteria and Assessment of the Effect of Salinity on Performance of a Denitrifying Microbial Fuel Cell, *Energies* **16** (2023) 877. https://doi.org/10.3390/en16020877

[6] R. Budiharjo, P. R. Sarjono, M. Asy'ari, Pengaruh Konsentrasi NaCl Terhadap Aktivitas Spesifik Protease Ekstraseluler dan Pertumbuhan Bakteri Halofilik Isolat Bittern Tambak Garam Madura, *Jurnal Kimia Sains dan Aplikasi* **20** (2017) 142-145. https://doi.org/10.14710/jksa.20.3.142-145 (In Indonesian)

[7] M. Christwardana, M. Saputra, M. Asy'ari, Exploring Halophilic Bacteria Bacillus clausii Isolated from Madura Salt Pond: Challenges of Utilization in Hypersaline Microbial Fuel Cells for Fish Processing Wastewater Treatment, *Applied Science and Engineering Progress* **18** (2025) 7663. https://doi.org/10.14416/j.asep.2025.01.003

[8] M. Christwardana, Khoirunnisa, M. Asy'ari, Evaluating nitrogen sources for enhanced halophilic bacteria growth, electron transfer, and microbial fuel cell performance, *Chemosphere* **378** (2025) 144397. https://doi.org/10.1016/j.chemosphere.2025.144397

[9] K. L. Dinh, C. T. Wang, H. N. Dai, V. M. Tran, M. L. P. Le, I. A. Saladaga, Y. A. Lin, Lactate and acetate applied in dual-chamber microbial fuel cells with domestic wastewater, *International Journal of Energy Research* **45** (2021) 10655-10666. https://doi.org/10.1002/er.6550

[10] W. Chen, Z. Liu, Y. Li, X. Xing, Q. Liao, X. Zhu, Improved electricity generation, coulombic efficiency and microbial community structure of microbial fuel cells using sodium citrate as an effective additive, *Journal of Power Sources* **482** (2021) 228947. https://doi.org/10.1016/j.jpowsour.2020.228947

[11] M. Christwardana, D. Frattini, G. Accardo, S. P. Yoon, Y. Kwon, Effects of methylene blue and methyl red mediators on performance of yeast based microbial fuel cells adopting polyethylenimine coated carbon felt as anode, *Journal of Power Sources* **396** (2018) 1-11. https://doi.org/10.1016/j.jpowsour.2018.06.005

[12] E. Laviron, General expression of the linear potential sweep voltammogram in the case of diffusionless electrochemical systems, *Journal of Electroanalytical Chemistry* **101** (1979) 19-28. https://doi.org/10.1016/S0022-0728(79)80075-3

[13] F. Mahmoodzadeh, N. Navidjouy, S. Alizadeh, M. Rahimnejad, Investigation of microbial fuel cell performance based on the nickel thin film modified electrodes, *Scientific Reports* **13** (2023) 20755. https://doi.org/10.1038/s41598-023-48290-3

[14] V. Babaeipour, S. A. Shojaosadati, R. Khalilzadeh, N. Maghsoudi, F. Tabandeh, A proposed feeding strategy for the overproduction of recombinant proteins in *Escherichia coli*, *Biotechnology and Applied Biochemistry* **49** (2008) 141-147. https://doi.org/10.1042/ba20070089

[15] B. Ughy, S. Nagyapati, D. B. Lajko, T. Letoha, A. Prohaszka, D. Deeb, A. Der, A. Pettko-Szandtner, L. Szilak, Reconsidering Dogmas about the Growth of Bacterial Populations, *Cells* **12** (2023) 1430. https://doi.org/10.3390/cells12101430
[16] S. Pinhal, D. Ropers, J. Geiselmann, H. De Jong, Acetate metabolism and the inhibition of bacterial growth by acetate, *Journal of Bacteriology* **201** (2019). https://doi.org/10.1128/JB.00147-19
[17] E. W. J. Van Niel, P.A.M. Claassen, A. J. M. Stams, Substrate and product inhibition of hydrogen production by the extreme thermophile, *Caldicellulosiruptor saccharolyticus, Biotechnology and Bioengineering* **81** (2003) 255-262. https://doi.org/10.1002/bit.10463
[18] X. S. Li, J. Z. Xue, Y. Qi, I. Muhammad, H. Wang, X. Y. Li, Y. J. Luo, D. M. Zhu, Y. H. Gao, L. C. Kong, H. X. Ma, Citric Acid Confers Broad Antibiotic Tolerance through Alteration of Bacterial Metabolism and Oxidative Stress, *International Journal of Molecular Sciences* **24** (2023) 9089. https://doi.org/10.3390/ijms24109089
[19] Q. Y. Ji, W. Wang, H. Yan, H. Qu, Y. Liu, Y. Qian, R. Gu, The Effect of Different Organic Acids and Their Combination on the Cell Barrier and Biofilm of *Escherichia coli*, *Foods* **12** (2023) 3011. https://doi.org/10.3390/foods12163011
[20] Z. Ullah, S. Zeshan, Effect of substrate type and concentration on the performance of a double chamber microbial fuel cell, *Water Science and Technology* **81** (2020) 1336-1344. https://doi.org/10.2166/wst.2019.387
[21] B. E. Logan, *Microbial Fuel Cells*, John Wiley & Sons, 2008. https://doi.org/10.1002/9780470258590
[22] Q. Wei, J. Zhang, F. Luo, D. Shi, Y. Liu, S. Liu, Q. Zhang, W. Sun, J. Yuan, H. Fan, H. Wang, L. Qi, G. Liu, Molecular mechanisms through which different carbon sources affect denitrification by Thauera linaloolentis: Electron generation, transfer, and competition, *Environment International* **170** (2022) 107598. https://doi.org/10.1016/j.envint.2022.107598
[23] J. A. Modestra, S. V. Mohan, Bio-electrocatalyzed electron efflux in gram positive and gram negative bacteria: an insight into disparity in electron transfer kinetics, *RSC Advances* **4** (2014) 34045-34055. https://doi.org/10.1039/C4RA03489A
[24] J. V. Boas, L. Peixoto, V. B. Oliveira, M. Simões, A. M. F. R. Pinto, Cyclic voltammetry study of a yeast-based microbial fuel cell, *Bioresource Technology Reports* **17** (2022) 100974. https://doi.org/10.1016/j.biteb.2022.100974
[25] B. J. Venton, Q. Cao, Fundamentals of fast-scan cyclic voltammetry for dopamine detection, *Analyst* **145** (2020) 1158-1168. https://doi.org/10.1039/c9an01586h
[26] N. Elgrishi, K. J. Rountree, B. D. McCarthy, E. S. Rountree, T. T. Eisenhart, J. L. Dempsey, A Practical Beginner's Guide to Cyclic Voltammetry, *Journal of Chemical Education* **95** (2018) 197-206. https://doi.org/10.1021/acs.jchemed.7b00361
[27] S. Ali, X. Zhang, M. S. Javed, X. Zhang, G. Liu, X. Wei, H. Chen, M. Imran, J. Wang, W. Han, J. Qi, 2H-MoS_2 nanosheets-based binder-free electrode material for supercapacitor, *Journal of Applied Physics* **132** (2022) 145001. https://doi.org/10.1063/5.0100522
[28] P. Wang, Y. Q. Qiu, X. T. Chen, X. F. Liang, L. H. Ren, Metabolomic insights into polyhydroxyalkanoates production by halophilic bacteria with acetic acid as carbon source, *Bioscience, Biotechnology, and Biochemistry* **83** (2019) 1955-1963. https://doi.org/10.1080/09168451.2019.1630252
[29] F. Orhan, Alleviation of salt stress by halotolerant and halophilic plant growth-promoting bacteria in wheat (Triticum aestivum), *Brazilian Journal of Microbiology* **47** (2016) 621-627. https://doi.org/10.1016/j.bjm.2016.04.001
[30] P. Nielsen, D. Fritze, F. G. Priest, Phenetic diversity of alkaliphilic Bacillus strains: Proposal for nine new species, *Microbiology* **141** (1995) 1745-1761. https://doi.org/10.1099/13500872-141-7-1745

[31] L. Zhou, T. Tang, D. Deng, Y. Wang, D. Pei, Isolation and Electrochemical Analysis of a Facultative Anaerobic Electrogenic Strain *Klebsiella* sp. SQ-1, *Polish Journal of Microbiology* **73** (2024) 143-153. https://doi.org/10.33073/pjm-2024-013

[32] J. Wang, M.F. He, D. Zhang, Z. Ren, T.S. Song, J. Xie, Simultaneous degradation of tetracycline by a microbial fuel cell and its toxicity evaluation by zebrafish, *RSC Advances* **7** (2017) 44226-44233. https://doi.org/10.1039/c7ra07799h

[33] X. Zhang, Y. Liu, L. Zheng, Q. Zhang, C. Li, Simultaneous degradation of high concentration of citric acid coupled with electricity generation in dual-chamber microbial fuel cell, *Biochemical Engineering Journal* **173** (2021) 108095. https://doi.org/10.1016/j.bej.2021.108095

[34] A. Pugazhendi, M. T. Jamal, B. A. Al-Mur, R. B. Jeyakumar, Bioaugmentation of electrogenic halophiles in the treatment of pharmaceutical industrial wastewater and energy production in microbial fuel cell under saline condition, *Chemosphere* **288** (2022) 132515. https://doi.org/10.1016/j.chemosphere.2021.132515

[35] M. T. Jamal, A. Pugazhendi, R. B. Jeyakumar, Application of halophiles in air cathode MFC for seafood industrial wastewater treatment and energy production under high saline condition, *Environmental Technology & Innovation* **20** (2020) 101119. https://doi.org/10.1016/j.eti.2020.101119

[36] A. Vijay, S. Arora, S. Gupta, M. Chhabra, Halophilic starch degrading bacteria isolated from Sambhar Lake, India, as potential anode catalyst in microbial fuel cell: A promising process for saline water treatment, *Bioresource Technology* **256** (2018) 391-398. https://doi.org/10.1016/j.biortech.2018.02.044

[37] A. Fathima, M. Z. H. bin Md Zoqratt, S. Y. Lim, F. Y. Ling, M. N. Chong, Influence of ferric oxides with varying crystallinity on the enrichment of halophilic exoelectrogens: An application for power generation in microbial fuel cells, *Journal of Water Process Engineering* **56** (2023) 104458. https://doi.org/10.1016/j.jwpe.2023.104458

[38] R. Gurav, S. K. Bhatia, T. R. Choi, H. R. Jung, S. Y. Yang, H. S. Song, Y. L. Park, Y. H. Han, J. Y. Park, Y. G. Kim, K. Y. Choi, Chitin biomass powered microbial fuel cell for electricity production using halophilic *Bacillus circulans* BBL03 isolated from sea salt harvesting area, *Bioelectrochemistry* **130** (2019) 107329. https://doi.org/10.1016/j.bioelechem.2019.107329

[39] J. L. Sanchez, D. Pinto, C. Laberty-Robert, Electrospun carbon fibers for microbial fuel cells: A novel bioanode design applied to wastewater treatment, *Electrochimica Acta* **373** (2021) 137864. https://doi.org/10.1016/j.electacta.2021.137864

J. Electrochem. Sci. Eng. **16** (2026) S3224

Open Access : : ISSN 1847-9286
https://pub.iapchem.org/ojs/index.php/JESE

Supplementary material to